New Sampling Strategies when Searching for Robust Solutions

Xin Fei, Jürgen Branke, *Member, IEEE*, Nalân Gülpınar

***Abstract*—Many real-world optimisation problems involve uncertainties, and in such situations it is often desirable to identify *robust* solutions that perform well over the possible future scenarios. In this paper, we focus on input uncertainty, such as in manufacturing, where the actual manufactured product may differ from the specified design but should still function well. Estimating a solution's expected fitness in such a case is challenging, especially if the fitness function is expensive to evaluate, and its analytic form is unknown. One option is to average over a number of scenarios, but this is computationally expensive. The archive sample approximation method reduces the required number of fitness evaluations by re-using previous evaluations stored in an archive. The main challenge in the application of this method lies in determining the locations of additional samples drawn in each generation to enrich the information in the archive and reduce the estimation error. In this paper, we use the Wasserstein distance metric to approximate the possible benefit of a potential sample location on the estimation error, and propose new sampling strategies based on this metric. Contrary to previous studies, we consider a sample's contribution for the entire population, rather than inspecting each individual separately. This also allows us to dynamically adjust the number of samples to be collected in each generation. An empirical comparison with several previously proposed archive-based sample approximation methods demonstrates the superiority of our approaches.**

***Index Terms*—Uncertainty, Average-case Robustness, Wasserstein Distance, Archive Sample Approximation.**

I. Introduction

GIVEN its ubiquity in many real-world problems, optimisation under uncertainty has gained increasing attention. Uncertainty may originate from various sources, such as imprecise model parameters or fluctuations in environmental variables. In the presence of uncertainty, it is often desirable to find a solution that is robust in the sense of performing well under a range of possible scenarios [1]. More specifically, our paper considers searching for robust solutions in the sense of high expected performance, given a distribution of disturbances to the decision variables. This is a typical scenario for example in manufacturing, where the actually manufactured products may differ from the design specification due to manufacturing tolerances.

Evolutionary algorithms (EAs) have been applied to solve various optimisation problems that involve uncertainties, see [2] for a survey. There are also different concepts related to robustness, including optimising the worst-case performance [3], robust optimisation over time [4], and active robustness [5]. The most widely researched robustness concept however, and the concept we consider in this paper, is to optimise a solution's expected fitness (often called effective fitness in the literature) over the possible disturbances [1].

To estimate an individual's effective fitness, sampling has been widely adopted in practice, and two sampling methods can be distinguished. *Implicit* sampling refers to the idea that because EAs are population-based, an over-evaluated individual due to a favourable disturbance can be counterbalanced by an under-evaluated neighbouring individual, and so simply increasing the population size should help guiding the EA in the right direction [6], [7]. In fact, as shown in [8], under the assumption of infinite population size and fitness-proportional selection, evaluating each solution at a single disturbed sample location instead of its actual location is equivalent to optimising the expected fitness directly. [7] proposed to increase the population size whenever the algorithm gets stalled. *Explicit* sampling, on the other hand, evaluates each individual multiple times and estimates its fitness as the average of the sampled evaluations. Obviously, while averaging over multiple evaluations increases the estimator accuracy, it is computationally rather expensive. A recent analytical study on the efficiency (progress rate) of implicit as well as explicit sampling-based evolution strategies can be found in [9].

Because of the large computational cost of sampling in case of expensive fitness functions, numerous studies have focused on allocating a limited sampling budget to improve the estimation accuracy, allowing to reduce the number of samples needed without degrading the performance of the EA. One possible approach for estimating effective fitness is to apply quadrature rules or variance reduction techniques [10]–[13]. Some authors observed that allocating samples in a manner that increases the probability of correct selection is more important than the accuracy of estimation [14], [15].

Another approach, called archive sample approximation (ASA), stores all past evaluations in a memory and uses this information to improve expected fitness estimates in future generations (for further information, refer to [10] and [16]). ASA can also be combined with the above sampling allocation methods to further enhance the accuracy of approximation. We have recently proposed an improved ASA method that uses the Wasserstein distance metric (a probability distance that quantifies the dissimilarity between two statistical objects) to identify the sample that is likely to provide the most valuable additional information to complement the knowledge available in the memory [17].

In this paper, we propose a Wasserstein-based archive sample approximation (WASA) framework. The sampling strategy in our previous study [17] is one of many possible approaches

Xin Fei, Jürgen Branke and Nalân Gülpınar are with Warwick Business School, The University of Warwick, Coventry CV4 7AL, UK.

in the WASA framework. Here, a new sampling strategy based on WASA is presented, which improves the performance in three ways:

1) A heuristic that considers what sample might provide the most valuable information for *all* individuals in the population *simultaneously*, thereby enhancing the performance of the final solution and accelerating the convergence of the EA toward a high-performance solution;
2) Introducing the concept of an approximation region that could improve the performance of the sampling strategy when few samples exist; and
3) Proposing a sample budget mechanism to adjust the sampling budget in the WASA framework.

The paper is structured as follows. Section II provides a brief overview of existing archive sample approximation methods. We then present our new approaches to allocating samples in Section III. These approaches are evaluated empirically using benchmark problems, and their performances are compared with other approaches in Section IV. The paper concludes with a summary and some ideas for future work.

II. Archive sample approximation

The problem of searching for robust solutions can be defined as follows. Consider an objective function $f : x \to \mathbb{R}$ with design variables $x \in \mathbb{R}^m$. The noise is defined on the probability space $(\Xi, \mathcal{B}(\Xi), \mathcal{P})$ where $\Xi = \prod_i^m [\ell_i, u_i]$ is a sample space, $\mathcal{B}(\Xi)$ is the Borel σ-algebra on Ξ and $\mathcal{P}$ is the probability measure on $\mathcal{B}(\Xi)$. For a particular solution x, location Z_x is random under this noisy environment, which is defined as:

$$Z_x = x + \xi, \quad \xi \in \Xi. \tag{1}$$

We then define the induced probability space for Z_x as $(D_x, \mathcal{B}(D_x), P_x)$, where D_x is the *disturbance region* as the set covering all possible locations as a result of disturbing solution x defined by:

$$D_x = \prod_{i=1}^{m} [x_i + \ell_i, x_i + u_i]; \tag{2}$$

and P_x is the probability measure defined so that, for $\phi \in \mathcal{B}(D_x)$,

$$P_x(\phi) = \mathcal{P}(Z_x^{-1}(\phi)). \tag{3}$$

Without loss of generality, for minimisation, the goal is to minimise the effective fitness, that is, the expected performance over the disturbance region as follows:

$$\min \quad f_{eff}(x) = \mathrm{E}[f(x)] = \int_{D_x} f(z) dP_x(z). \tag{4}$$

As the fitness formulation is unknown in many industrial applications, the integral cannot be computed directly. In practice, we can numerically compute this integral using sampling techniques. Let $\hat{Z}_x = \{z_n | \ n \in N\}$ be the realisations of random location Z_x. The empirical probability measure (i.e. probability distribution) of these samples is a discrete probability measure, which can be defined so that, for $\phi \in \mathcal{B}(\hat{Z}_x)$,

$$\hat{P}_x(\phi) = \frac{1}{|N|} \sum_{n \in N} \mathbb{1}_\phi(z_n), \tag{5}$$

where $\mathbb{1}_\phi(\cdot)$ is the indicator function. If the sample size $|N|$ is sufficiently large, the effective fitness can be well estimated as follows:

$$f_{eff}(x) \approx \sum_{n \in N} f(z_n) \hat{P}_x(z_n). \tag{6}$$

However, if evaluating the fitness function is computationally expensive, this may not be possible.

The ASA approach originally proposed in [18] saves previously evaluated points in the search space and their corresponding fitness values in an archive $\mathcal{A}$. Generally, the archive $\mathcal{A}$ is a set of ordered pairs (z, ρ), where z is the sample location and ρ is its fitness value. The archive information can be reused when estimating the expected fitness of a new solution. ASA performs three main steps during a fitness evaluation.

1) The previously evaluated points which are in the solution's *disturbance region* are retrieved from the archive. Given the disturbance region D_x, the available archive information can be identified as
$$\mathcal{A}_x = \{(z, \rho) \in \mathcal{A} | \ z \in Z_x\}.$$
2) A *sampling strategy* is used to determine at what additional locations samples should be collected. Let C_x denote the new sample locations. It is desirable to select a set of sample points C_x which maximise our knowledge of the fitness landscape in the disturbance region.
3) All samples located within the disturbance region D_x need to be assigned probabilities. Then, the estimated effective fitness $\hat{f}_{eff}(x)$ can be calculated as
$$\hat{f}_{eff}(x) = \underbrace{\sum_{a \in \mathcal{A}_x} a^{(2)} Q_x(a^{(1)})}_{\text{Archive information}} + \underbrace{\sum_{c \in C_x} f(c) Q_x(c)}_{\text{New information}}$$
where $Q_x(\cdot)$ is the point probability; $a^{(1)}$ and $a^{(2)}$ represent the first and second elements of the ordered pair in the archive $\mathcal{A}_x$.

The overall procedure integrating ASA into an EA is visualised in Fig. 1.

In the simplest ASA, the sampling strategy randomly evaluates new points within the disturbance region and assigns equal probabilities to all available samples, see, e.g., [10]. However, if the distribution of available samples in the disturbance region is not representative of Z_x, the resulting estimation of effective fitness may be very biased. In an attempt to fill "holes" in the disturbance region, the authors in [16], [19] and [20] proposed to iteratively pick a sample point that has maximal distance from any archive sample point in the disturbance region.

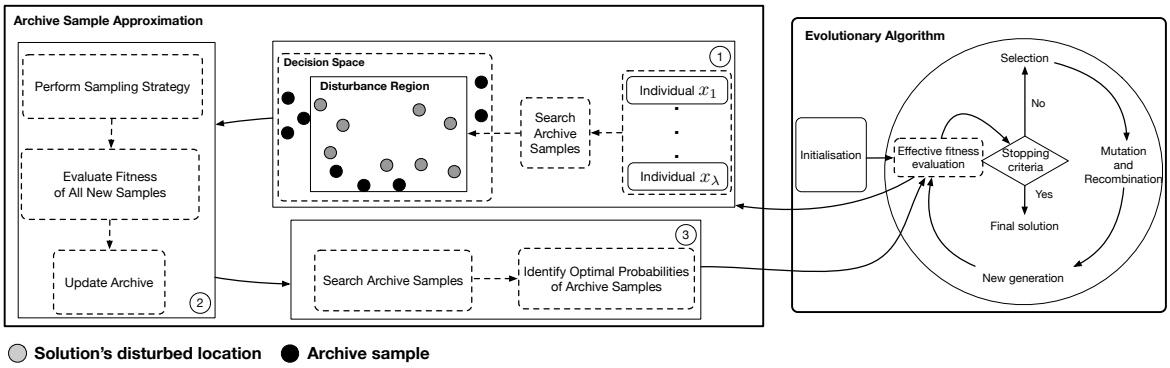

Fig. 1. Illustration of integrating ASA into an EA.

III. The Wasserstein-based archive sample approximation

Given the archive samples, we aim to provide an accurate estimation of effective fitness for each individual by sampling additional locations. The estimation error with respect to effective fitness is defined as follows:

$$e_{eff}(x) = |f_{eff}(x) - \hat{f}_{eff}(x)|. \tag{7}$$

In reality, estimation error cannot be computed given that the actual effective fitness $f_{eff}(x)$ is unknown. Therefore, we use Wasserstein distance as an upper bound approximation for the estimation error. We call this framework Wasserstein-based archive sample approximation.

In the following subsections, we first introduce the formulation of Wasserstein distance, explain the principle behind WASA and describe the underlying sampling problem of WASA. Then, we enhance the description of the sampling strategy used in our previous work [17] and propose a new population-based myopic sampling strategy.

A. The Wasserstein Distance Metric

The Wasserstein distance metric (also known as the Earth mover's distance) is a statistical distance between two probability measures, which can be computed by solving the Monge-Kantorovich transportation problem [21]. The two probability measures in the Wasserstein distance are considered as warehouses and destinations. The distance value between two probability measures is determined by the minimum transportation cost from warehouses to destinations.

More formally, let ϱ and ν be probability measures with samples $G = \{g_j |\ j \in J\}$ and $H = \{h_k |\ k \in K\}$, and corresponding probabilities $\{\varrho_j |\ j \in J\}$ and $\{\nu_k |\ k \in H\}$, respectively. Let Ψ denote the set of all joint measures with marginal measures ϱ and ν. The Wasserstein distance metric between ϱ and ν can be formulated as

$$\begin{aligned} &W(\varrho, \nu) \doteq \\ &\min_{\psi \in \Psi} \sum_{k \in K} \sum_{j \in J} d(g_j, h_k)\psi(\varrho_j, \nu_k) \\ &s.t. \sum_{j \in J} \psi(\varrho_j, \nu_k) = \nu_k,\ \forall k \\ &\sum_{k \in K} \psi(\varrho_j, \nu_k) = \varrho_j,\ \forall j \\ &\psi(\varrho_j, \nu_k) \geq 0,\ \forall j, k, \end{aligned} \tag{8}$$

where the distance $d(g_j, h_k)$ between locations g_j and h_k is measured by the Euclidean distance i.e.,

$$d(g_j, h_k) = \|g_j - h_k\|_2. \tag{9}$$

Different from other divergence measures such as the Kullback-Leibler divergence, the Wasserstein distance works on arbitrary sets and doesn't assume that one random set is a subset of another. The reader is referred to [22] for further information on the Wasserstein distance metric.

B. The Upper Bound Approximation for Estimation Error

As discussed in Section II, the effective fitness of a particular solution can be numerically computed by using a set of samples. If the number of samples is large enough, the corresponding empirical probability measure will converge to the actual probability. Given that the computational cost of evaluating a sample is expensive, we aim to approximate this "large" empirical probability measure with a "smaller" discrete probability measure. The challenge is how to estimate the corresponding estimation error. Since the actual effective fitness cannot be computed in practice, the estimation error cannot be obtained directly.

In this paper, we provide an upper bound approximation of the estimation error (stated in Theorem 1) that can be calculated without requiring any fitness information.

Theorem 1: Suppose that we have two discrete probability measures ν and ϱ. The effective fitness is numerically computed by using the probability measure ϱ; and ν is the

probability measure approximating ϱ. If the fitness function $f : x \to \mathbb{R}$ is Lipschitzian, then the estimation error satisfies

$$\left| \sum_{j \in J} f(g_j)\varrho_j - \sum_{k \in K} f(h_k)\nu_k \right| \leq \alpha \; W(\varrho, \nu) \tag{10}$$

where α is a positive constant.

Proof: See Appendix A of the online supplement. □

Theorem 1 implies that the estimation error with respect to two discrete probability measures can be upper bounded by the Wasserstein distance. For practical applications, the fitness function in the disturbance region might be intermittent or non-Lipschitz. In this case, the aforementioned upper bound still holds if two probability measures are identical.

C. The Modified Wasserstein Distance Metric

Before explaining the WASA framework, we introduce a modified Wasserstein distance metric used in sample sets with known and unknown probabilities. The probability ν is assumed to be unknown. This metric provides the optimal probability measure $\{\nu_j |\; j \in J\}$, which results in the smallest Wasserstein distance value. We define the modified Wasserstein distance metric $M(G, H)$ between two samples G and H as follows,

$$\begin{aligned} M(G,H) = \min_{\nu_k} \quad & W(\varrho, \nu) \doteq \\ \min_{\psi \in \Psi, \nu_k} \quad & \sum_{k \in K} \sum_{j \in J} d(g_j, h_k)\psi(\varrho_j, \nu_k) \\ s.t. \quad & \sum_{k \in K} \psi(\varrho_j, \nu_k) = \varrho_j, \;\; \forall j \\ & \sum_{k \in K} \nu_k = 1, \nu_k \geq 0, \;\; \forall k \\ & \psi(\varrho_j, \nu_k) \geq 0, \;\; \forall j, k. \end{aligned} \tag{11}$$

Note that the computational cost for solving the above optimisation problem is high for a large-scale distance comparison. However, when the strong duality property holds, the objective values of the dual and primal problems are identical, which can be used to solve the optimisation problem (11).

Let η_j for $j \in J$ denote a vector of dual decision variables assigned to the first set of constraints of problem (11) by ignoring the second set of constraints. Then, the dual problem for (11) can be derived as,

$$\begin{aligned} M(G,H) = \max_{\eta_j} \quad & \sum_{j \in J} \varrho_j \eta_j \\ s.t. \quad & \eta_j \leq d(g_j, h_k), \;\; \forall j, k. \end{aligned} \tag{12}$$

Due to the special structure of inequality in the constraints of the dual problem (12), the optimal decision variables η_j^* can be easily determined. The optimal dual decision is the minimum Euclidean distance from the sample h_k to the sample g_j, and can be calculated as

$$\eta_j^* = \min_{h_k} \; d(g_j, h_k), \quad \forall j. \tag{13}$$

Once the optimal dual decision variable η_j^* has been determined, the Wasserstein distance $M(G, H)$ can be computed as

$$M(G,H) = \sum_{j \in J} \varrho_j \eta_j^*. \tag{14}$$

Additionally, the probability measure ν can be computed as

$$\nu_k = \sum_{j \in J} \mathbb{1}_{g_j}(h_k)\varrho_j, \;\; \forall k \tag{15}$$

where $\mathbb{1}_{g_j}(h_k)$ is an indicator function and defined as

$$\mathbb{1}_{g_j}(h_k) = \begin{cases} 1, & \text{if } h_k \text{ is the closest sample to } g_j \\ 0, & \text{otherwise.} \end{cases} \tag{16}$$

The overall procedure for efficiently computing the modified Wasserstein distance value is described in Algorithm 1.

Algorithm 1 Efficient method for computing $M(G, H)$

Inputs:

- Samples $G = \{g_j | j \in J\}$ with probabilities $\{\varrho_j | j \in J\}$
- Samples $H = \{h_k |\; k \in K\}$.

Outputs:

- Modified Wasserstein distance value $M(G, H)$.
- Optimal probabilities $\{\nu_k^* |\; k \in K\}$ for samples H.

for $j \in J, k \in K$ **do**
  Compute Euclidean distance $d(g_j, h_k)$ using (9).
end for
for $j \in J$ **do**
  Find the optimal dual solution η_j^* using (13).
end for
Compute the distance value $M(G, H)$ via (14).
Compute the optimal probabilities $\{\nu_k^* |\; k \in K\}$ as in (15).

D. The WASA Sampling Problem

In this subsection, we introduce the sampling problem in WASA. Let x_l for $l \in \Lambda = \{1, \ldots, \lambda\}$ denote the l-th individual from a particular population during the EA search process. Using similar notation as in Section II, let Z_l for $l \in \Lambda$ be the random location of individual x_l, which is defined on the probability space $(D_l, \mathcal{B}(D_l), P_l)$. We then generate a large set $\hat{Z}_l = \{z_{n,l} \in D_l |\; n \in N\}$ from the random location Z_l to represent the disturbed locations of each individual. The empirical probability measure of these disturbed locations is denoted by $\hat{P}_l$. Note that these large sample sets are used only when computing the Wasserstein distance value and as a set of candidates for evaluation.

Given an archive $\mathcal{A}$ that consists of previously evaluated solutions, the available archive samples for individual x_l can be retrieved as follows:

$$\mathcal{A}_l = \{(z, \rho) \in \mathcal{A} |\; z \in D_l\}. \tag{17}$$

Then, the previously evaluated sample locations S_l can be identified as

$$S_l = \{a^{(1)} |\; a \in \mathcal{A}_l\}. \tag{18}$$

The *optimal sampling problem* is to minimise the total effective fitness estimation error over all individuals at the present EA's generation by searching:

- the best additional sample locations C_l; and
- the optimal probability measure Q_l on $\mathcal{B}(C_l \cup S_l)$

We can formulate the aforementioned problem by using the following optimisation model:

$$\begin{aligned}
&\min_{C_l, Q_l} \quad \sum_{l\in\Lambda} e_{eff}(x_l) = \sum_{l\in\Lambda} |f_{eff}(x_l) - \hat{f}_{eff}(x_l)| \\
&s.t. \quad f_{eff}(x_l) = \sum_{n\in N} f(z_{n,l})\hat{P}_l(z_{n,l}), \forall l \\
&\hat{f}_{eff}(x_l) = \sum_{a\in\mathcal{A}_l} a^{(2)} Q_l(a^{(1)}) + \sum_{c\in C_l} f(c) Q_l(c), \forall l \\
&\sum_{a\in\mathcal{A}_l} Q_l(a^{(1)}) + \sum_{c\in C_l} Q_l(c) = 1,\ Q_l(\cdot) \geq 0, \forall l \\
&\sum_{l\in\Lambda} |C_l| = B,\ C_l \subseteq \hat{Z}_l, \forall l.
\end{aligned} \tag{19}$$

As previously discussed, some fitness information in (19) is unavailable. Therefore, the optimal sampling problem cannot be directly solved. By applying Theorem 1, we approximate the optimal sampling problem by using the Wasserstein distance as follows:

$$\begin{aligned}
\min_{C_l, Q_l} \sum_{l\in\Lambda} W(\hat{P}_l, Q_l) = \min_{C_l} \sum_{l\in\Lambda} M(\hat{Z}_l, C_l \cup S_l) \\
s.t. \sum_{l\in\Lambda} |C_l| = B, C_l \subseteq \hat{Z}_l, \forall l
\end{aligned} \tag{20}$$

where B is the evaluation budget. This new approximate formulation is referred to as the WASA sampling problem. The details of derivation of the optimisation model (20) are provided in Appendix B of the online supplement.

Essentially, we minimise the upper bound approximation of the estimation error in order to provide heuristic sample locations without requiring any fitness information. Although the WASA sampling problem is a nonlinear and non-convex optimisation problem, it is still solvable. The optimal solution for this approximate problem formulation can be found by repeatedly solving the following four related steps:

1) Fixing the cardinality $|C_l|$ for $l \in \Lambda$ such that $\sum_{l\in\Lambda} |C_l| = B$.
2) Selecting the new samples C_l from $\hat{Z}_l$.
3) Constructing the sample set Y_l for each individual x_l as follows,
$$Y_l = S_l \cup C_l,\ \forall l. \tag{21}$$
4) Computing the modified Wasserstein distance value $M(\hat{Z}_l, Y_l)$ for $l \in \Lambda$ by applying Algorithm 1 to solve the following optimisation model.
$$\begin{aligned}
&\min_{Q_l, \psi_l} \sum_{z\in\hat{Z}_l} \sum_{y\in Y_l} d(z,y)\psi_l(\hat{P}_l(z), Q_l(y)) \\
&s.t. \quad \sum_{y\in Y_l} \psi_l(\hat{P}_l(z), Q_l(y)) = \hat{P}_l(z),\ \forall z \in \hat{Z}_l \\
&\qquad \sum_{y\in Y_l} Q_l(y) = 1,\ Q_l(y) \geq 0,\ \forall y \in Y_l \\
&\qquad \psi_l(z,y) \geq 0,\ \forall z \in \hat{Z}_l, y \in Y_l.
\end{aligned} \tag{22}$$

Generally, the optimal solution of the WASA sampling problem cannot be obtained within a reasonable time. For instance, there exist two individuals x_1 and x_2 at a particular EA's iteration. Consider that the cardinalities of $\hat{Z}_1$ and $\hat{Z}_2$ are 200. Given the sampling budget $B = 2$, we have three ways to allocate this sampling budget to x_1 and x_2.

$$(|C_1|, |C_2|) \in \{(1,1), (2,0), (0,2)\}.$$

If we should take one sample from $\hat{Z}_1$ and one form $\hat{Z}_2$, then we have $40,000$ sample combinations. In case of taking two samples from $\hat{Z}_1$ or two from $\hat{Z}_2$, $19,900$ combinations are found. This basically results in $79,800$ repetitions for performing the four related steps to find the optimal solution. The small case shows that heuristic approaches to solve the WASA sampling problem are needed.

In the next subsection, we introduce two Wasserstein-based sampling strategies aimed at efficiently making sampling decisions for the above WASA sampling problem.

E. Equal Fixed Sampling Strategy

A straightforward way to simplify the WASA sampling problem is to consider each individual separately, and allocate to each individual the same fixed number of new samples. We call this strategy Equal Fixed Sampling (EFS). The sampling budget in EFS must be an integral multiple of the number of individuals. EFS is an iterative method that determines one new sample point at each step. Algorithm 2 describes the overall procedure of incorporating the EFS strategy into WASA.

For individual x_l, EFS first retrieves previously evaluated information $\mathcal{A}_l$ from the archive $\mathcal{A}$ and identifies the archive sample locations S_l by using (18). Then, EFS constructs the candidate sets $Y_{n,l}$ for $n \in N$ by uniting one of the individual's disturbed locations $z_{n,l}$ with archive points as follows:

$$Y_{n,l} = z_{n,l} \cup S_l,\ \forall n \in N. \tag{23}$$

EFS evaluates the modified Wasserstein distance value $V_{EFS}(z_{n,l})$ of each disturbed location $z_{n,l}$ as

$$V_{EFS}(z_{n,l}) \doteq M(Y_{n,l}, \hat{Z}_l),\ \forall n \in N. \tag{24}$$

EFS next selects and evaluates the new sample point z^* resulting in the smallest value, i.e.,

$$z^* = \arg\min\{V_{EFS}(z_{n,l})|\ n \in N\}. \tag{25}$$

The fitness of this point is evaluated and the new sample information will be added into the archive $\mathcal{A}$. The process repeats until the algorithm runs out of sampling budget for this individual.

When this iterative process has been completed, EFS retrieves the archive samples $\mathcal{A}_l^*$ from the *updated* archive. The previously evaluated sample locations for the individual x_l can be identified as follows,

$$Y_l^* = \{a^{(1)}|\ a \in \mathcal{A}_l^*\}. \tag{26}$$

Now we compute the optimal probabilities Q_l for Y_l^* by using (22). Then, the estimated effective fitness of each individual can be calculated as

$$\hat{f}_{eff}(x_l) = \sum_{a \in \mathcal{A}_l^*} a^{(2)} Q_l(a^{(1)}). \tag{27}$$

Algorithm 2 The procedure of including EFS into WASA

Inputs:
- Set of disturbed locations $\hat{Z}_l = \{z_{n,l} | \ n \in N\}$ with empirical probability measure $\hat{P}_l$ for $l \in \Lambda$.
- Sampling budget B.
- Archive $\mathcal{A}$.

Outputs:
- Estimated effective fitness $\hat{f}_{eff}(x_l)$ for $l \in \Lambda$.

for $l \in \Lambda$ **do**
  Retrieve archive information A_l using (17).
  Identify sample locations S_l from A_l as in (18).
  for $b \in \{1, \ldots, B/\lambda\}$ **do**
    for $n \in N$ **do**
      Construct the candidate set $Y_{n,l}$ using (23).
      Compute the $V_{EFS}(z_{n,l})$ value via (24).
    end for
    Find $z^* = \arg\min\{V_{EFS}(z_{n,l}) | \ n \in N\}$.
    Evaluate the fitness of the best location $f(z^*)$.
    Update the archive $\mathcal{A} \leftarrow \mathcal{A} \cup (z^*, f(z^*))$.
  end for
end for
for $l \in \Lambda$ **do**
  Retrieve the archive information A_l^* as in (17).
  Construct the archive sample set Y_l^* via (26).
  Calculate the probability measure $\hat{P}_l$ on Y_l^* using (22).
  Compute the effective fitness $\hat{f}_{eff}(x_l)$ as in (27).
end for

Fig. 2 illustrates EFS by using a $2D$ example. Let us consider the solution located at $(0, 0)$, which is represented as a grey solid hexagon, assume the sampling budget of this solution is one, and the disturbance region is from -1 to 1 in x- and y-directions. We approximate the disturbance region by using Latin hypercube sampling to generate 6 disturbances. The corresponding disturbed locations of this solution are represented by grey solid circles. In the disturbance region, there are two archive points which are depicted as black solid circles. We now calculate the V_{EFS} value of each disturbed location. The results are shown in Fig. 2 (a). We can find that the best sample point is the grey solid circle whose V_{EFS} value is 0.8486. Fig. 2 (b) describes how to determine the probabilities of samples used to estimate the effective fitness. The probability of each disturbed location is 0.1667 because the total number of disturbed locations is six in this example. The black solid circle located at $(0.1600, 0.2000)$ is the point closest to the grey solid circle $(-0.1863, 0.1745)$. According to probability re-allocation rules (15), the new probability for this black solid circle is 0.1667. The new sample point marked by a triangle is the best representation of the two grey solid circles. However, the new probability of this point is 0.5000 because this point is also the nearest to itself. The new probabilities of the other black solid circles can be assigned following the same procedure.

F. Population-based Myopic Sampling Strategy

EFS may spend unnecessary sampling on an individual that already has a small Wasserstein distance value but ignores the needs of an individual with large Wasserstein distance value. This inefficient sampling allocation frequently appears in the search process because of the exploration and exploitation strategies used in the EAs. The current promising area on the decision space is exploited repeatedly, and the archive set already contains adequate information for approximating the effective fitness landscape of individuals in this area. However, the archive does not contain information on previously unexplored areas, and in those areas new sampling is indispensable.

To alleviate this problem, we propose here population-based myopic sampling (PMS). The key idea is to allow sampling, at each step, the disturbed location of any individual that greatly minimises the average Wasserstein distance over the entire population. This sampling strategy is particularly effective when disturbance regions partially overlap one another, because one additional sample point might contribute to improving the fitness estimate for several individuals. PMS furthermore introduces the concept of an approximation region which may be chosen different from the disturbance region and allows the use of archive samples also outside the immediate disturbance region. Finally, since the budget in a generation no longer needs to be a multiple of the population size, we introduce a mechanism to adapt the sampling budget of each generation depending on the change in the average Wasserstein distance over the entire population. Algorithm 3 describes the overall procedure of including PMS into WASA. In the following, we present the core ingredients of PMS, including approximation region, myopic sampling location selection, and sampling budget adjustment.

1) Approximation region: Generally, ASA begins with the search of available archive points which are located within the individual's disturbance region. If the archive contains only a small number of available points, it may improve the estimation of the effective fitness to additionally include archive points slightly outside the disturbance region. In PMS, we call this enlarged region *approximation region*. Let $\mathcal{R}_l$ denote the approximation region of individual x_l. Given the sample space Ξ of noise, the size of approximation region $\mathcal{R}_l$ is controlled by a parameter κ ($\kappa \geq 1$), which is defined as follows,

$$\mathcal{R}_l = \{x_l + \varsigma | \ \varsigma \in \prod_{i=1}^{m} [\kappa * \ell_i, \kappa * u_i]\}. \tag{28}$$

Obviously, the larger κ, the more archive samples are used for fitness estimation. On the other hand, if κ is chosen too large, the archive points may be located too far from the individual's disturbance region, thereby causing unpredictable errors in effective fitness estimation. So, κ needs to be chosen carefully.

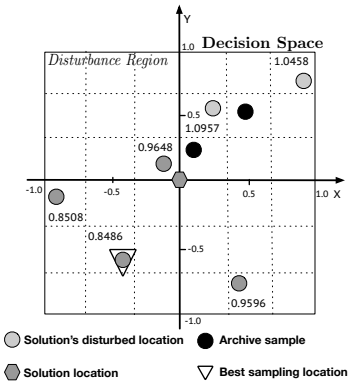

(a) Selection process in EFS.

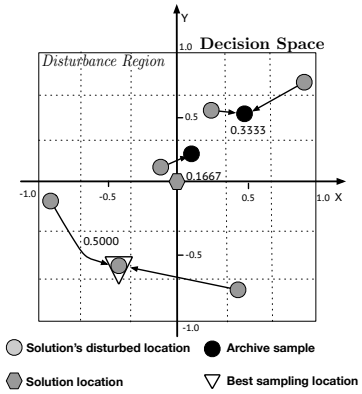

(b) Probability assignment in EFS.

Fig. 2. Description of using EFS.

Algorithm 3 The procedure of including PMS into WASA

Inputs:

- Set of disturbed locations $\hat{Z}_l = \{z_{n,l} | \ n \in N\}$ with empirical probability measure $\hat{P}_l$ for $l \in \Lambda$.
- Sampling budget $B \in [B_{lower}, B_{upper}]$.
- Archive $\mathcal{A}$.
- Approximation region parameter κ.
- Average Wasserstein distance $\bar{W}^{t-1}$.

Outputs:

- Estimated effective fitness $\hat{f}_{eff}(x_l)$ for $l \in \Lambda$.
- Average Wasserstein distance $\bar{W}^t$.

Initialise $b \leftarrow 0$.
for $l \in \Lambda$ **do**
  Set approximation region $\mathcal{R}_l$ via (28).
end for
while $b < B_{upper}$ **do**
  Retrieve archive samples A_l for $l \in \Lambda$ using (17).
  Identify sample locations S_l from A_l for $l \in \Lambda$ via (18).
  for $l \in \Lambda, n \in N$ **do**
    for $m \in \Lambda$ **do**
      Construct the candidate set $Y_{l,n,m}$ as in (29).
    end for
    Compute the $V_{PMS}(z_{n,l})$ value via (30).
  end for
  Find $z^* = \arg\min\{V_{PMS}(z_{n,l}) | \ n \in N, l \in \Lambda\}$.
  Evaluate the fitness of the best location $f(z^*)$.
  Update the archive $\mathcal{A} \leftarrow \mathcal{A} \cup (z^*, f(z^*))$.
  Compute the $\bar{W}^t$ value using (33).
  if $\bar{W}^{t-1} > \bar{W}^t$ and $b > B_{lower}$ **then**
    $b = B_{upper}$ //Stop sampling.
  else
    Set $b \leftarrow b + 1$.
  end if
end while
for $l \in \Lambda$ **do**
  Retrieve the archive information A_l^* as in (17).
  Construct the archive sample set Y_l^* via (26).
  Calculate the probability measure $\hat{P}_l$ on Y_l^* using (22).
  Compute the effective fitness $\hat{f}_{eff}(x_l)$ as in (27).
end for

Fig. 3 illustrates the benefit of including additional archive points. The solution is located at $(0, 0)$, whilst its disturbance region is from -1 to 1 in x- and y-directions. The black solid circles denote the archive points, among which three are located within and two outside the disturbance region. The grey solid circles represent the disturbed locations of this solution. If we restrict ASA to the disturbance region, the minimum Wasserstein distance we can obtain from the two black solid points and one grey solid point to be additionally evaluated is 2.276. If we set the approximation region parameter κ as 120%, the grey squiggle in Fig. 3 denotes the extension region with respect to the solution's disturbance region. Two additional archive points can be used to estimate effective fitness. Accordingly, the best Wasserstein distance value we can obtain from the four black and one grey points reduces to 1.2935. This example demonstrates that an enlarged approximation region may reduce the Wasserstein distance.

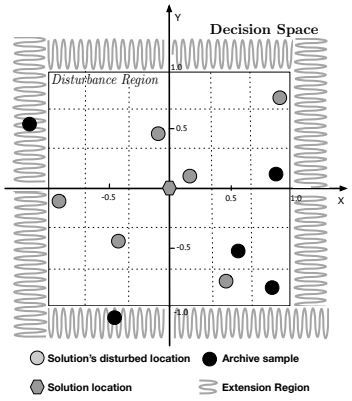

Fig. 3. Using approximation region in WASA.

2) Myopic sampling location selection: Given the archive samples of each individual, PMS myopically selects the best sampling point. This myopic strategy iteratively builds candidate sets by combining a new sample at one disturbed location of any individual with the archive samples of any individual, as described in the following equation:

$$Y_{l,n,m} = z_{n,l} \cup S_m, \tag{29}$$

with $n \in N$, $m \in \Lambda$ and $l \in \Lambda$. The myopic selection criterion is based on the average Wasserstein distance for the entire population. Let $V_{PMS}(z_{n,l})$ represent the average modified Wasserstein distance value by sampling the disturbed location $z_{n,l}$. Then, we can write the $V_{PMS}(z_{n,l})$ value as follows:

$$V_{PMS}(z_{n,l}) = \sum_{m \in \Lambda} \mathbb{1}_{\mathcal{R}_m}(z_{n,l}) M(Y_{l,n,m}, \hat{Z}_m) \tag{30}$$

where $\mathbb{1}_{\mathcal{R}_m}(z_{n,l})$ is an indicator function, defined as

$$\mathbb{1}_{\mathcal{R}_m}(z_{n,l}) = \begin{cases} 1, & \text{if } z_{n,l} \in \mathcal{R}_m \\ 0, & \text{otherwise} \end{cases} \tag{31}$$

that controls that a sample only contributes to an individual's Wasserstein distance calculation if it is within its approximation region.

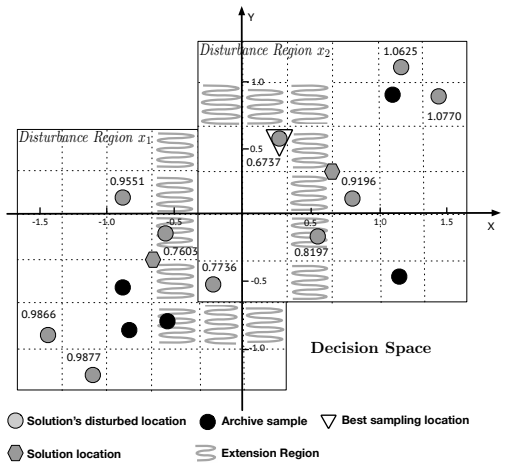

Fig. 4. The V_{PMS} value computation in PMS.

Fig. 4 explains how to compute the V_{PMS} value in the PMS strategy. As shown in Fig. 4, two candidate solutions x_1 and x_2 are respectively located at $(-0.666, -0.333)$ and $(0.666, 0.333)$. The disturbance region of each solution is represented by 6 Latin hypercube samples (grey solid circles). The approximation region parameter κ is set to be 130%. The grey squiggle is the extension region with respect to the disturbance region. Given the budget to sample one new point, we need to determine which grey point is the best sampling location for these two solutions (x_1 and x_2) when it is combined with the archive points (black). Note that the grey points outside the overlapped approximation region, for instance, $(-1.5340, -0.6312)$, only contribute to one solution. The V_{PMS} value for each grey point is shown in Fig. 4. It can be observed that the sample location $(0.3000, 0.5100)$ (triangle) allows for the smallest average Wasserstein distance for these two solutions.

3) Sampling budget adjustment: PMS allows the automatic reduction of the sampling budget used during an iteration of the EA if the archive already provides plenty of information on candidate individuals. The sampling budget is adaptively determined by the average Wasserstein distance over all individuals. We attempt to decrease this average distance monotonously. Considering a progressing evolution, we like to derive improved estimates for effective fitness. Given $V_{PMS}(z_{n,l})$ for $n \in N$ and $l \in \Lambda$, the best sampling location can be identified as follows:

$$z^* = \arg\min\{V_{PMS}(z_{n,l}) |\ n \in N, l \in \Lambda\}. \tag{32}$$

Then, we can compute the average modified Wasserstein distance $\bar{W}$ at the current population t as follows:

$$\bar{W}^t = \sum_{l \in \Lambda} \mathbb{1}_{\mathcal{R}_l}(z^*) M(z^* \cup S_l, \hat{Z}_l) + (1 - \mathbb{1}_{\mathcal{R}_l}(z^*)) M(S_l, \hat{Z}_l). \tag{33}$$

PMS stops sampling for the current population when the current average Wasserstein distance using the usable samples is less than the recorded average Wasserstein distance of the previous population $t-1$. In other words,

$$\bar{W}^t < \bar{W}^{t-1}. \tag{34}$$

In practical use, we suggest to assign lower and upper limits for the number of new samples evaluated in each iteration. The lower limit ensures that a minimum additional knowledge on the underlying fitness landscape is collected in each iteration. It also prevents getting permanently stuck in an artificial optimum of a false approximation model. The upper bound prevents the spending of a large number of samples in the current population. Given that EAs are iterative search methods, the samples must also be allocated to the future population rather than extensively sampling the fitness for the current population.

IV. Empirical Results

In this section, we examine the effect of varying algorithmic parameters on the performance of the PMS strategy. Moreover, we empirically compare the WASA strategies with several other ASA approaches from the literature using a variety of benchmark problems with different landscape features as well as a real-life robust design problem. All results are averaged over 30 independent runs with different random seeds.

A. Experimental Setup for Artificial Benchmark Problems

1) Overview of Artificial Benchmark Problems: We have chosen six artificial benchmark problems from the literature, their mathematical formulations can be found in Appendix C of the online supplement. Fig. 5 provides one-dimensional visualisations of the original and effective fitness landscapes. The test problems have different characteristics:

- **TP 1**, taken from [23], has a discontinuous unimodal original fitness landscape. The peaks of the original and effective fitness landscapes are asymmetric and located next to each other. This problem characteristic can test an algorithm's ability to precisely identify the peak of effective fitness at the discontinuous landscape.
- **TP 2**, adopted from [23], can be viewed as the continuous version of TP 1.
- **TP 3**, adopted from [18], has multimodal original and effective fitness landscapes. The global optimum of the original fitness $(x = 1)$ is a local optimum of the effective fitness landscape, and vice versa. Poor effective fitness

estimates in the early phase of optimisation may misdirect the EA towards the wrong region.
- **TP 4**, taken from [23], has two global minima in the effective fitness landscape. The global minimum of the original fitness is a local maximum of the effective fitness.
- **TP 5**, adapted from [23], combines the problem characteristics of TP 2 and TP 3.
- **TP 6**, taken from [8], has the global minima of the effective fitness landscape as being the local minima of the original fitness landscape.

2) Evolutionary Algorithm: Essentially, the archive-based approximation is a part of the EA's fitness evaluation procedure. Therefore, it is straightforward to integrate our proposed sampling strategies into any evolutionary algorithm. We have adopted the covariance matrix adaptation evolution strategy (CMA-ES) for the experiments. CMA-ES is implemented based on the MATLAB toolbox [24]. We have modified the fitness evaluation procedure in this toolbox and integrated the various sampling strategies. The used parameter settings of the CMA-ES toolbox are listed in Table I.

TABLE I
THE CMA-ES PARAMETER SETTINGS

CMA-ES Parameters	Selected Settings
(μ, λ)	(4,8)
initial standard deviation	$\frac{1}{4}$ search interval width
recombination	equally weighted recombination
initial point	centre of search interval
total number of evaluations	$1,600$

3) Solution Selection & Performance Measure: We employ the best observed individual, i.e. the individual with best estimated effective fitness, at the final generation as the solution that would be reported to the decision-maker. The actual effective fitness of the selected solution is evaluated by $10,000$ Monte-Carlo samples generated from the underlying noise. Moreover, we look at the algorithm's convergence and the average effective fitness over the whole run. Ideally, we would expect the sampling approach to have a fast convergence and to provide a high-quality solution at the final generation.

4) Disturbance Generation for WASA: The performance of WASA is closely associated with the way the approximate uncertainty set $\hat{Z}_l$ is generated. We use 243 Latin hypercube disturbances for all individuals within a generation, which reduces the variance in comparing the effective finesses in an uncertain environment. To avoid over-fitting to a specific set of disturbances, we change the set of disturbances at each iteration of the EA.

B. Performance of the PMS Strategy Depending on Approximation Region Parameter

We numerically study the effect of using various approximation region parameters (κ=100%, 120% and infinity). The lower and upper limits of the sampling budget at each iteration are fixed at 4 and 8, respectively. Fig. 6 presents the convergence of the average effective fitness of the best observed solution.

As can be seen, the convergence towards high-performance solutions can be accelerated by using a proper approximation region parameter. Given the same amount of evaluations, PMS-120% performs better than PMS-100%. The superiority of using PMS-120% is significant before $1,000$ evaluations, because early in the run, information in the archive is sparse, and the wider approximation region can use more archive samples in the individual's effective fitness estimation. At the end of the run, the PMS-120% strategy is able to find better solutions than all other strategies in all test problems, indicating that a proper setting of the approximation region prevents CMA-ES from early convergence towards local optima by incorporating more archive samples in the effective fitness estimation.

In all benchmark problems, the average effective fitness of using PMS-infinity deteriorates during the first 100 evaluations, though this value is improved quickly at later evaluations. The reason is that the new sampling locations determined by PMS-infinity are always located at the centre of a cluster of individuals when the archive is empty or contains only few samples, which actually misleads the EA search process. This negative effect becomes serious in test problems TP 5 and TP 6, because the problem characteristics demand that the robust approach is able to identify the correct search area early on. Otherwise, the EA search process converges towards local optima.

To support Fig. 6, Table II reports on the average effective fitness obtained over all $1,600$ evaluations of the run. Again, we can observe that PMS-120% provides the fastest convergence pattern among these three strategies for all test functions. PMS-infinity displays good convergence in TP 1, 2 and 4. Additionally, Table III presents the performance of the final solution at the end of the EA search process. These results show that PMS-120% has the best performance in all benchmark problems, and PMS-infinity presents a performance advantage over PMS-100%. However, PMS-infinity performs worse than PMS-120% in most of the test functions. The results confirm the theoretical ground discussed in Section III, namely that a moderate increase of the approximation region beyond the disturbance region is useful, but too much may lose its benefit.

TABLE II
AVERAGE EFFECTIVE FITNESS OVER 1,600 EVALUATIONS

Test Problem	Mean ± Std. err.		
	PMS-100%	PMS-120%	PMS-infinity
TP 1	0.150±0.003	**0.140±0.003**	**0.145±0.002**
TP 2	0.674±0.014	**0.634±0.014**	**0.651±0.014**
TP 3	0.901±0.015	**0.848±0.025**	0.890±0.021
TP 4	**0.192±0.001**	**0.190±0.001**	**0.191±0.001**
TP 5	0.528±0.009	**0.495±0.018**	0.527±0.022
TP 6	0.458±0.006	**0.452±0.006**	0.469±0.008

Best results and those statistically not different from best are highlighted in bold.

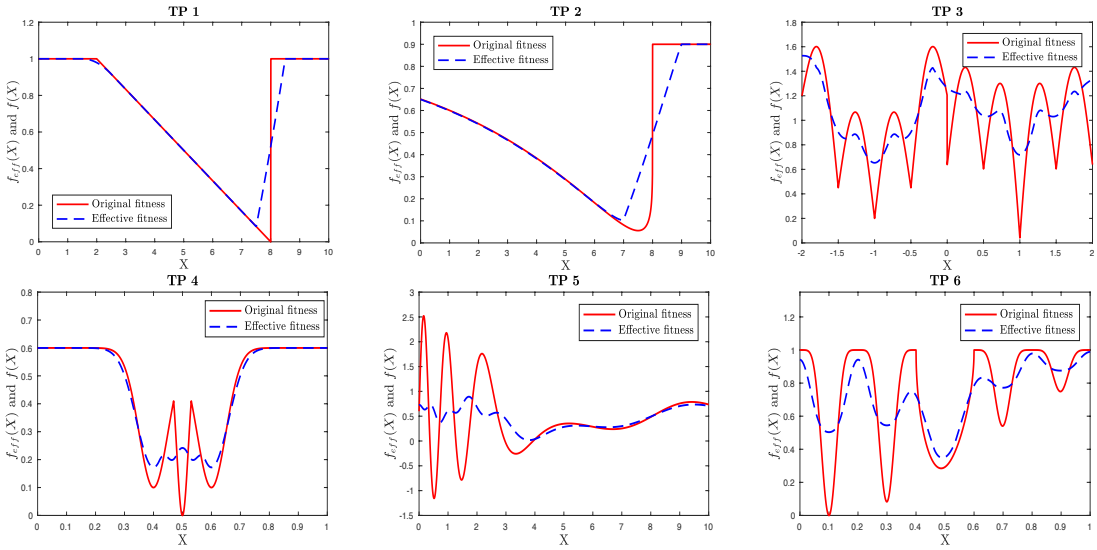

Fig. 5. 1-D visualisation of original and effective fitness of the 5-D test problems. Solid line: original fitness landscape. Dash line: effective fitness landscape.

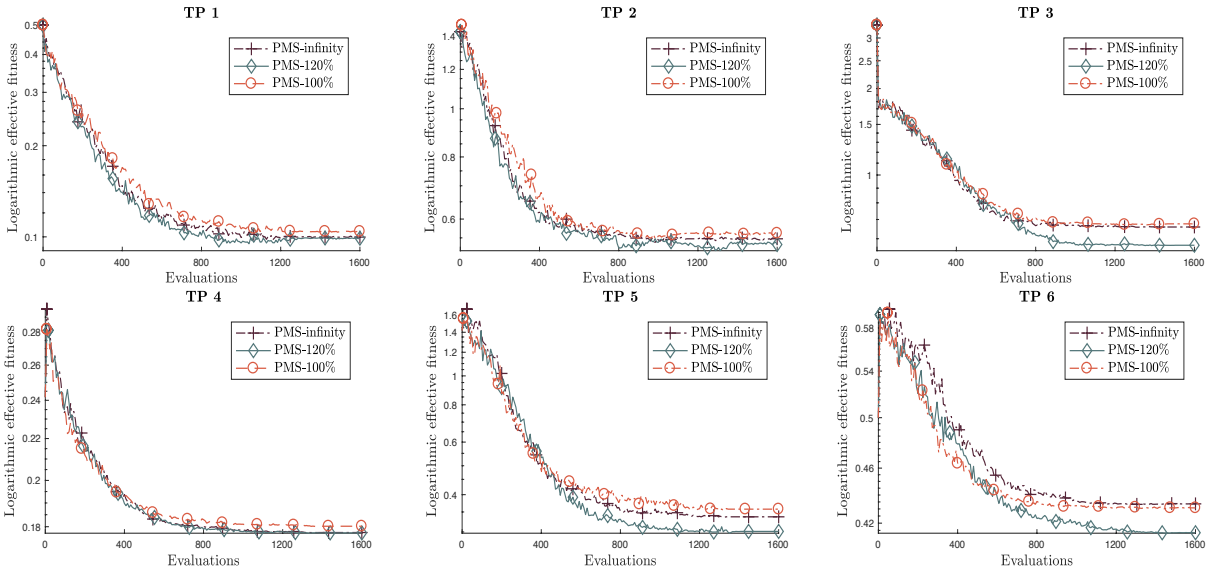

Fig. 6. Convergence comparison with respect to evaluations for various approximation region parameters.

TABLE III
EFFECTIVE FITNESS OF THE SOLUTION AT 1,600 EVALUATIONS

Test Problem	Mean ± Std. err.		
	PMS-100%	PMS-120%	PMS-infinity
TP 1	**0.104±0.006**	**0.098±0.002**	**0.099±0.001**
TP 2	0.561±0.007	**0.533±0.006**	0.548±0.005
TP 3	0.676±0.031	**0.569±0.022**	0.659±0.027
TP 4	0.182±0.002	**0.177±0.002**	**0.177±0.001**
TP 5	0.358±0.011	**0.301±0.009**	0.337±0.004
TP 6	0.431±0.009	**0.413±0.006**	0.436±0.007

Best results and those statistically not different from best are highlighted in bold.

C. Performance of the PMS Strategy with Various Sampling Budget Limits

In this experiment, we investigate the convergence pattern with varying lower and upper sampling budget limitations. We consider the setting where the sampling budget per generation is allowed to change between 4 and 8 as default, which is abbreviated as the PMS-$[4, 8]$ strategy. We firstly test the effect of rising the lower limit of PMS-$[4, 8]$. As such, we consistently use 8 evaluations throughout the search process and denote this strategy as PMS-$[8, 8]$. Secondly, we study the impact of increasing the upper limit on the convergence behaviour. Therefore, we include PMS-$[4, 10]$ in this experiment, whose upper limit is set to 10. The approximation region is fixed at 120% of each direction of an individual's perturbed region. Fig. 7 displays the results of the various sampling strategies for all test problems.

As shown in Fig. 7, PMS-$[4, 8]$ and PMS-$[8, 8]$ have similar convergence patterns at early search iterations because both strategies implement eight evaluations when the archive has few usable samples. Nevertheless, the convergence of PMS-$[4, 8]$ becomes faster than that of PMS-$[8, 8]$ once the

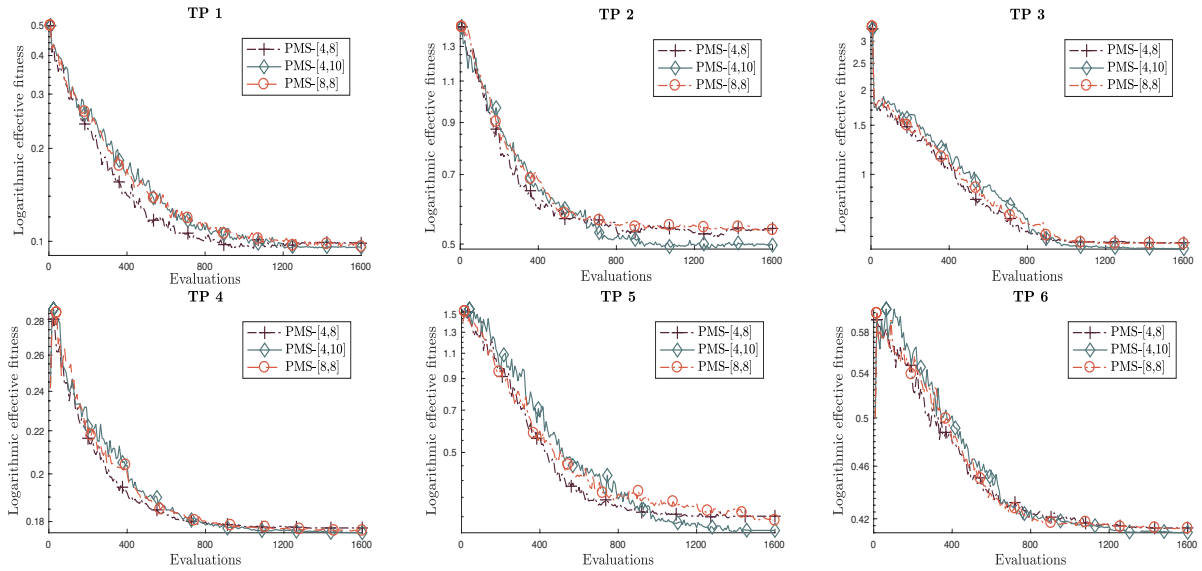

Fig. 7. Convergence comparison with the evaluations for various sampling budget limits.

archive has a sufficient number of samples, indicating that PMS-$[4, 8]$ saves evaluations when the average Wasserstein distance is monotonously decreasing anyway. Moreover, we observe that the convergence of PMS-$[4, 10]$ is slow at early iterations. This is because PMS-$[4, 10]$ is allowed to spend more evaluations exploring the correct search directions at early iterations.

TABLE IV
AVERAGE EFFECTIVE FITNESS OVER 1,600 EVALUATIONS

Test Problem	Mean ± Std. err. PMS-$[4, 8]$	PMS-$[4, 10]$	PMS-$[8, 8]$
TP 1	**0.140±0.003**	0.152±0.002	0.151±0.003
TP 2	**0.634±0.014**	**0.628±0.012**	**0.629±0.005**
TP 3	**0.848±0.025**	0.897±0.021	**0.876±0.027**
TP 4	**0.190±0.001**	0.194±0.001	0.193±0.001
TP 5	**0.495±0.018**	0.540±0.029	0.514±0.028
TP 6	**0.452±0.006**	**0.457±0.008**	**0.453±0.008**

Best results and those statistically not different from best are highlighted in bold.

TABLE V
EFFECTIVE FITNESS OF THE SOLUTION AT 1,600 EVALUATIONS

Test Problem	Mean ± Std. err. PMS-$[4, 8]$	PMS-$[4, 10]$	PMS-$[8, 8]$
TP 1	0.098±0.002	**0.094±0.001**	**0.093±0.003**
TP 2	0.533±0.006	**0.498±0.009**	0.535±0.002
TP 3	**0.569±0.022**	**0.542±0.028**	**0.565±0.031**
TP 4	**0.177±0.002**	**0.175±0.001**	**0.176±0.001**
TP 5	0.301±0.009	**0.269±0.018**	**0.294±0.016**
TP 6	**0.413±0.006**	**0.410±0.008**	**0.413±0.008**

Best results and those statistically not different from best are highlighted in bold.

Again, Table IV and V summarise the overall performance and the effective fitness value of the final solution, respectively. We observe that strategies PMS-$[4, 8]$ and PMS-$[8, 8]$ perform similarly at the end of EA search process, but PMS-$[4, 8]$ converges faster than PMS-$[8, 8]$, indicating that our sampling budget adjustment can save evaluations without sacrificing the performance of the final solution. PMS-$[4, 10]$ provides the best final solution in all test problems, but converges more slowly.

D. Average Performance Comparison

We verify the performance of the proposed strategies, namely EFS and PMS, by comparing with the following archive-based approaches from the literature:

1) **SEM**: The strategy randomly samples one location within the individual's perturbed area [8].
2) **SEMAR**: This is the SEM strategy integrated with the archive sample approximation strategy [18].
3) **ABRSS**: This strategy is based on an archive sample approximation approach consisting of two main steps. For each disturbed location, the first step is to identify the closest sample point in the archive, and the second step is to check whether this disturbed location is also the closest disturbed location of its selected archive sample point [16]. If this is the case, the selected archive sample point will be used in the effective fitness estimation; otherwise, this disturbed location will be considered for an additional sampling.
4) **ABRSS+OP**: This strategy implements ABRSS to determine the additional sample points, but assigns the optimal probabilities that are obtained from the modified Wasserstein distance for all sample points involved in the effective fitness estimation.

Note that all sampling strategies are inserted into the same CMA-ES, so that all performance differences can be attributed to the sampling strategy alone.

The PMS strategy sets the approximation region parameter κ as 120% and fixes the lower and upper limits for the number of samples per iteration at 4 and 8, respectively. Fig. 8 displays the computational results of using various bounds for the sampling budget. Moreover, in Fig. 9, we report the average estimation error over the course of the run, which is defined

by the mean squared error between the true and estimated effective fitness.

As shown in Fig. 8, the SEM approach provides the worst results for all test problems, because this approach does not use an archive and one new sample is not sufficient to estimate the effective fitness. Compared to SEM, the archive-based approaches show a good convergence on most test problems. SEMAR and ABRSS exhibit similar convergence behaviour on most test problems. Since the ABRSS+OP approach implements the optimal probabilities, its convergence is faster than ABRSS and SEMAR in the most of test problems. Nevertheless, ABRSS+OP performs worse than the WASA-based strategies, i.e., EFS and PMS, indicating that the Wasserstein distance metric provides an advantage in selecting good sampling locations. Additionally, the results demonstrate the good performance of PMS which converges faster than EFS over the first $1,000$ evaluations in all problems.

The effective fitness of the best observed solution obtained from various strategies averaged over $1,600$ evaluations is reported in Table VI. The results confirm the importance of good sampling strategy design. We find that the WASA sampling strategies converge faster than other methods. For strategies PMS and EFS, we observe that the convergence of PMS is more rapid than EFS for all test problems except TP 2 and 6. Table VII displays the performance of the final solution obtained from various approaches. The result once again confirms the superiority of WASA sampling strategies and the performance advantage of PMS over EFS.

The results of average estimation error in Fig. 9 confirm our findings from previous convergence comparisons. The SEM approach consistently exhibits large effective fitness estimation errors. The SEMAR and ABRSS strategies reduce the average estimation error when the number of evaluations is small, because they reuse past sampling information. However, SEMAR and ABRSS lack a good mechanism to determine the probability weights for the samples used in the effective fitness estimation. This deficiency might lead to biases in the estimation. In some cases, the average estimation errors of SEMAR and ABRSS are actually increasing over the run. By contrast, the approaches that adopt optimal probabilities, i.e. ABRSS+OP, EFS and PMS, keep decreasing the average estimation error throughout the run; and PMS is the fastest approach in decreasing the average estimation error.

E. Robust Multi-point Airfoil Shape Optimisation under Uncertain Manufacturing Errors

Finally, we test the proposed strategies on a simple real-world problem. We consider a multi-point airfoil shape optimisation problem with manufacturing errors. Although advances in high-performance computing have reduced the CPU time with respect to the performance evaluation of airfoil shape, this robust optimisation problem still requires a significant computational effort because algorithms might need thousands of evaluations under various possible manufacturing errors. Therefore, it is an ideal testbed for examining the performance of various sampling approaches under the condition of limited evaluation budget.

We consider the subsonic 2-D airfoil design problem, which is a variant obtained from [3]. The baseline shape is NACA 0012 airfoil [25], which is illustrated in Fig. 10. We implement 10 Hicks-Henne bump functions [26] $f_i(z)$ for $i = 1, \ldots, 10$ with the upper and lower surfaces of NACA 0012 (denoted as $y_u^b(z)$ and $y_l^b(z)$) to parameterise the upper surface $y_u(z)$ and the lower surface $y_l(z)$. They are defined as follows:

$$y_u(z) = y_u^b(z) + \sum_{i=1}^{6} \theta_i f_i(z)$$

and

$$y_l(z) = y_l^b(z) + \sum_{i=7}^{10} \theta_i f_i(z),$$

where z is a non-dimensional abscissa, and θ_i is the design variable on the i-th Hicks-Henne bump function. These Hicks-Henne bump functions combined with design variables can be used to tune the upper and lower surfaces. The definitions of Hicks-Henne bump functions and the ranges of the design variables can be found in Appendix D of the online supplement.

The "fitness" of the airfoil shape is defined as the average lift-to-drag ratio over three flow velocities ($\mathbf{M}_1 = 0.5$ mach, $\mathbf{M}_2 = 0.55$ mach and $\mathbf{M}_3 = 0.6$ mach) when Reynolds number (Re) and Angle of Attack (AoA) are $300,000$ and 4°, respectively. Thus, the fitness function $f(\theta)$ can be written as follows:

$$\begin{aligned}
&f(\theta) = \frac{1}{3}(C_1 + C_2 + C_3)\\
&\text{where}\\
&C_1 = C_{L/D}(\mathbf{M}_1, Re, AoA, \theta_1, \cdots, \theta_{10})\\
&C_2 = C_{L/D}(\mathbf{M}_2, Re, AoA, \theta_1, \cdots, \theta_{10})\\
&C_3 = C_{L/D}(\mathbf{M}_3, Re, AoA, \theta_1, \cdots, \theta_{10})
\end{aligned}$$

where $C_{L/D}$ denotes the lift-to-drag ratio. We assume that all design variables are affected by uniformly disturbed manufacturing errors. The range of manufacturing error for all design variables is fixed as $[-0.001, 0.001]$. The overall robust design problem can be formulated as

$$\begin{aligned}
&\max \quad f_{eff}(\theta) = \mathbb{E}[f(\theta + \xi)] = \frac{1}{3}(C_1 + C_2 + C_3)\\
&\text{where}\\
&C_1 = C_{L/D}(\mathbf{M}_1, Re, AoA, \theta_1 + \xi_1, \cdots, \theta_{10} + \xi_{10})\\
&C_2 = C_{L/D}(\mathbf{M}_2, Re, AoA, \theta_1 + \xi_1, \cdots, \theta_{10} + \xi_{10})\\
&C_3 = C_{L/D}(\mathbf{M}_3, Re, AoA, \theta_1 + \xi_1, \cdots, \theta_{10} + \xi_{10})\\
&\xi_i \in \mathcal{U}(-0.001, 0.001), \quad i = 1, \ldots, 10.
\end{aligned}$$

In this experiment, the airfoil shape of lift-to-drag ratios at various Mach numbers are evaluated by Drela's XFOIL [27]. This software is an open-source aerodynamic analysis package for subsonic isolated airfoils, which allows the use of relatively lower computational effort than advanced CFD programs. For this problem, we fix the (μ, λ) parameters in CMA-ES at $(5, 10)$ and choose the total evaluations as 1,200. The lower and upper limits of the evaluation budget at each iteration for the PMS strategy are fixed at 5 and 10, respectively;

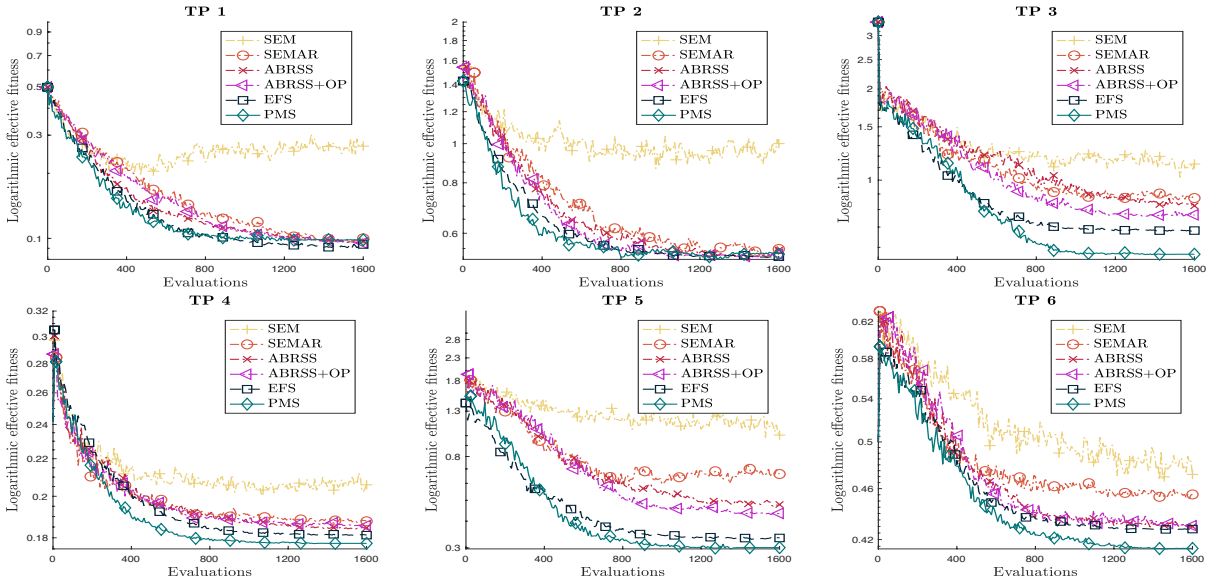

Fig. 8. Convergence comparison of different sampling strategies with respect to evaluations.

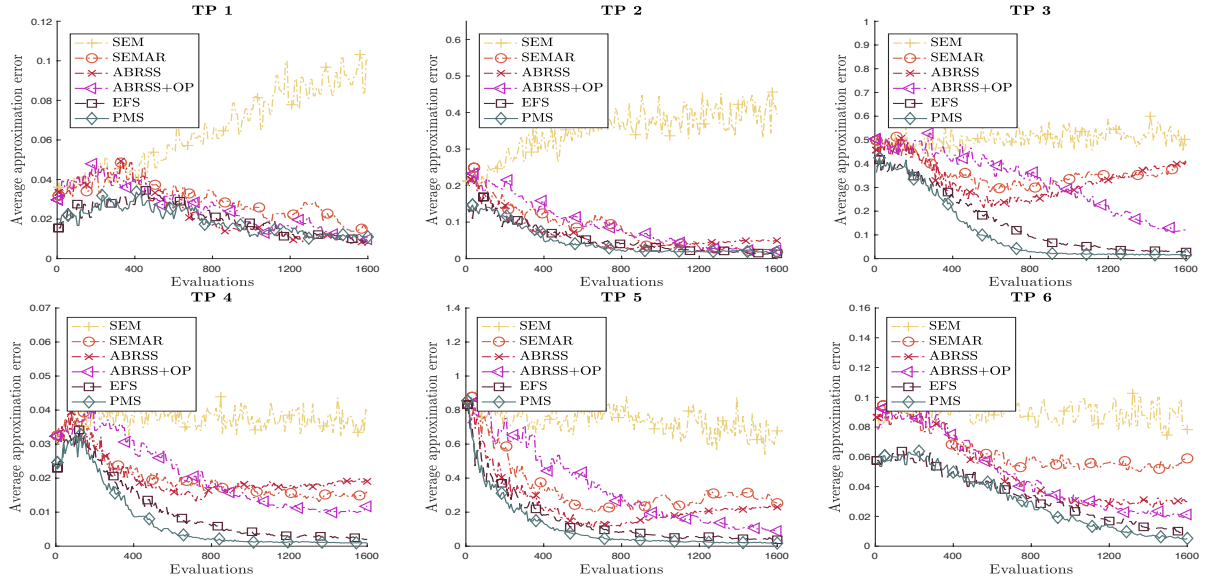

Fig. 9. Average estimation error comparison of different sampling strategies with respect to evaluations.

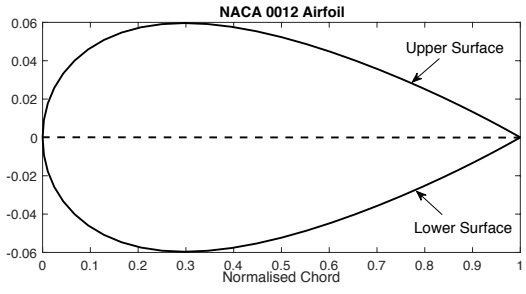

Fig. 10. The baseline shape of the robust design problem.

whereas the evaluation budget of other sampling approaches is fixed at 10, that is, each solution is evaluated once. The other experimental setup is exactly same as in previous experiments.

Fig. 11 shows the convergence of the average effective fitness of the currently best solution based on the estimated effective fitness values.

As can be seen in Fig. 11, the convergence of WASA sampling strategies is considerably faster than other sampling approaches, which clearly confirms the superiority of WASA sampling strategies in this real-world problem. The non-WASA sampling strategies (SEM, SEMAR, ABRSS and ABRSS+OP) exhibit similar convergence patterns. For EFS and PMS, the solutions at 400 evaluations are even better than the solutions obtained from the other sampling approaches after $1,200$ evaluations. In comparison to EFS, we observe that PMS provides a good convergence rate at the first 200 evaluations due to its advanced sample selection method in the WASA framework, which is consistent with the results of

TABLE VI
AVERAGE EFFECTIVE FITNESS OVER 1,600 EVALUATIONS

Test Problem	Mean ± Std. Err. SEM	SEMAR	ABRSS	ABRSS+OP	EFS	PMS
TP 1	0.260±0.006	0.171±0.007	0.156±0.004	0.160±0.006	0.144±0.003	**0.140±0.003**
TP 2	1.018±0.008	0.728±0.017	0.702±0.017	0.676±0.010	**0.625±0.015**	**0.634±0.014**
TP 3	1.304±0.024	1.121±0.035	1.164±0.031	1.012±0.040	0.902±0.035	**0.848±0.025**
TP 4	0.213±0.001	0.199±0.001	0.200±0.001	0.198±0.001	0.196±0.001	**0.190±0.001**
TP 5	1.280±0.010	0.853±0.021	0.783±0.022	0.753±0.031	0.497±0.018	**0.495±0.018**
TP 6	0.519±0.007	0.485±0.008	0.471±0.008	0.474±0.011	**0.462±0.007**	**0.452±0.006**

Best results and those statistically not different from best are highlighted in bold.

TABLE VII
EFFECTIVE FITNESS OF THE SOLUTION AT 1,600 EVALUATIONS

Test Problem	Mean ± Std. Err. SEM	SEMAR	ABRSS	ABRSS+OP	EFS	PMS
TP 1	0.267±0.020	**0.100±0.006**	**0.098±0.003**	**0.096±0.006**	**0.095±0.003**	**0.098±0.002**
TP 2	1.000±0.052	0.548±0.011	0.554±0.024	**0.535±0.007**	**0.528±0.002**	**0.533±0.006**
TP 3	1.131±0.075	0.873±0.054	0.823±0.071	0.769±0.042	0.682±0.031	**0.569±0.022**
TP 4	0.205±0.004	0.187±0.009	0.184±0.003	0.185±0.002	**0.181±0.003**	**0.177±0.002**
TP 5	1.005±0.076	0.662±0.044	0.479±0.057	0.434±0.053	0.335±0.012	**0.301±0.009**
TP 6	0.471±0.013	0.455±0.011	0.429±0.009	0.430±0.011	0.428±0.005	**0.413±0.006**

Best results and those statistically not different from best are highlighted in bold.

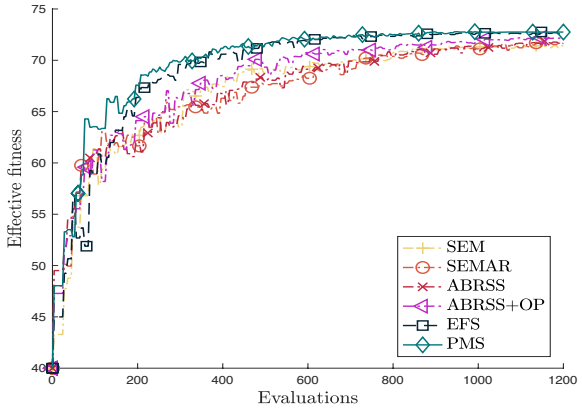

Fig. 11. Convergence comparison of various sampling strategies with respect to evaluations in the robust airfoil shape optimisation problem.

artificial test functions presented in Section IV.D.

Table VIII reports both the average effective fitness over 1,200 evaluations (abbreviated as A.E.F.) and the effective fitness of the solution at 1,200 evaluations (abbreviated as E.F.). The results show that PMS provides the fastest convergence among the six approaches. The convergence of EFS is worse than that of PMS but still much better than those of the non-WASA approaches. The optimal probabilities used in the effective fitness estimation have improved performance of ABRSS+OP in this test problem. Compared to ABRSS and SEMAR, ABRSS+OP has a faster convergence and provides better final solutions, though it is still worse than the WASA sampling strategies.

TABLE VIII
PERFORMANCE OF VARIOUS SAMPLING APPROACHES IN THE ROBUST AIRFOIL SHAPE OPTIMISATION PROBLEM

Method	Mean ± Std. Err. A.E.F.	E.F.
SEM	67.665±0.434	71.410±0.434
SEMAR	66.140±1.011	71.657±0.305
ABRSS	66.359±0.721	71.638±0.311
ABRSS+OP	67.742±0.987	72.035±0.277
EFS	68.453±0.239	72.614±0.089
PMS	**69.257±0.233**	**72.780±0.068**

Best results and those statistically not different from best are highlighted in bold.

V. CONCLUSION

When using evolutionary algorithms to search for a robust solution, estimating the effective fitness is challenging. Storing previous evaluations in an archive and using this information to improve the fitness estimate, the so-called archive sample approximation method, has been proposed by several authors to improve the estimation accuracy without increasing the sampling budget. A crucial part of ASA is the sampling strategy, i.e., to decide what new solutions should be evaluated. In this paper, we used the Wasserstein distance metric to approximate an upper bound for the error and proposed two Wasserstein-based sampling strategies to suggest promising sampling locations. Minimizing the upper bound cannot guarantee minimization of the actual error, however, knowing that we have no information on the fitness function apart from previous samples, it is a promising approach. One sampling strategy considers the sampling contribution from each individual's perspective, and allocates an equal number of evaluations to each individual. The second strategy approximates the sampling contribution for all individuals. The empirical results on various benchmark problems and robust airfoil shape optimisation demonstrate the benefit of using Wasserstein-based sampling strategies and the advantage of considering the population contribution in the sampling strategy design.

This study can be further developed in several possible directions. The idea of sampling budget control could be refined, with more sophisticated control strategies. The approximation region is only really helpful in the beginning of

the run, so parameter κ controlling the extension could be reduced over the run. The idea should be tested also with other distributions for the disturbances. It also would be interesting to compare WASA with surrogate-based approaches. The Wasserstein distance metric might even be helpful in constructing better surrogate models. Finally, the development of WASA to address more complex real-world applications would be valuable.

ACKNOWLEDGMENT

This research utilised Queen Mary's MidPlus computational facilities, supported by QMUL Research-IT and funded by EPSRC grant EP/K000128/1.

REFERENCES

[1] H.-G. Beyer and B. Sendhoff, "Robust optimization – a comprehensive survey," *Computer Methods in Applied Mechanics and Engineering*, vol. 196, no. 33, pp. 3190 – 3218, 2007.
[2] Y. Jin and J. Branke, "Evolutionary optimization in uncertain environments-a survey," *IEEE Transactions on Evolutionary Computation*, vol. 9, no. 3, pp. 303–317, 2005.
[3] Y.-S. Ong, P. B. Nair, and K. Y. Lum, "Max-min surrogate-assisted evolutionary algorithm for robust design," *IEEE Transactions on Evolutionary Computation*, vol. 10, no. 4, pp. 392–404, 2006.
[4] H. Fu, B. Sendhoff, K. Tang, and X. Yao, "Robust optimization over time: Problem difficulties and benchmark problems," *IEEE Transactions on Evolutionary Computation*, vol. 19, no. 5, pp. 731–745, 2015.
[5] S. Salomon, G. Avigad, R. C. Purshouse, and P. J. Fleming, "Gearbox design for uncertain load requirements using active robust optimization," *Engineering Optimization*, vol. 48, no. 4, pp. 652–671, 2016.
[6] M. Rattray and J. Shapiro, "Noisy fitness evaluation in genetic algorithms and the dynamics of learning," in *Foundations of Genetic Algorithms*. Morgan Kaufmann, 1997, pp. 117–139.
[7] H.-G. Beyer and B. Sendhoff, "Evolution strategies for robust optimization," in *2006 IEEE International Conference on Evolutionary Computation*, 2006, pp. 1346–1353.
[8] S. Tsutsui and A. Ghosh, "Genetic algorithms with a robust solution searching scheme," *IEEE Transactions on Evolutionary Computation*, vol. 1, no. 3, pp. 201–208, 1997.
[9] H.-G. Beyer and B. Sendhoff, "Towards a steady-state analysis of an evolution strategy on a robust optimization problem with noise-induced multi-modality," *IEEE Transactions on Evolutionary Computation*, vol. 21, no. 4, pp. 629–643, 2017.
[10] J. Branke, C. Schmidt, and H. Schmeck, "Efficient fitness estimation in noisy environments," in *Proceedings of the 3rd Annual Conference on Genetic and Evolutionary Computation*. Morgan Kaufmann, 2001, pp. 243–250.
[11] A. Di Pietro, L. While, and L. Barone, "Applying evolutionary algorithms to problems with noisy, time-consuming fitness functions," in *Proceedings of the 2004 Congress on Evolutionary Computation*, vol. 2, 2004, pp. 1254–1261.
[12] B. Huang and X. Du, "A robust design method using variable transformation and gauss-hermite integration," *International Journal for Numerical Methods in Engineering*, vol. 66, no. 12, pp. 1841–1858, 2006.
[13] S. H. Lee, W. Chen, and B. M. Kwak, "Robust design with arbitrary distributions using gauss-type quadrature formula," *Structural and Multidisciplinary Optimization*, vol. 39, no. 3, pp. 227–243, 2009.
[14] P. Stagge, "Averaging efficiently in the presence of noise," in *International Conference on Parallel Problem Solving from Nature*. Springer, 1998, pp. 188–197.
[15] J. Branke and C. Schmidt, "Selection in the presence of noise," in *Proceedings of the 2003 International Conference on Genetic and Evolutionary Computation*. Springer, 2003, pp. 766–777.
[16] J. Kruisselbrink, M. Emmerich, and T. Bäck, "An archive maintenance scheme for finding robust solutions," in *International Conference on Parallel Problem Solving from Nature*. Springer, 2010, pp. 214–223.
[17] J. Branke and X. Fei, "Efficient sampling when searching for robust solutions," in *International Conference on Parallel Problem Solving from Nature*. Springer, 2016, pp. 237–246.
[18] J. Branke, *Evolutionary optimization in dyamic environments*. Kluwer, 2001.
[19] A. Saha, T. Ray, and Smith, "Towards practical evolutionary robust multi-objective optimization," in *2011 IEEE Congress of Evolutionary Computation*, 2011, pp. 2123–2130.
[20] A. Cervantes, D. Quintana, and G. Recio, "Efficient dynamic resampling for dominance-based multiobjective evolutionary optimization," *Engineering Optimization*, vol. 49, no. 2, pp. 311–327, 2017.
[21] C. Villani, *Optimal transport: old and new*. Springer, 2008, vol. 338.
[22] P. Billingsley, *Probability and measure*. John Wiley & Sons, 2008.
[23] I. Paenke, J. Branke, and Y. Jin, "Efficient search for robust solutions by means of evolutionary algorithms and fitness approximation," *IEEE Transactions on Evolutionary Computation*, vol. 10, no. 4, pp. 405–420, 2006.
[24] N. Hansen, "CMA-ES source code." [Online]. Available: https://www.lri.fr/ hansen/cmaesintro.html
[25] I. H. Abbott and A. E. Von Doenhoff, *Theory of wing sections, including a summary of airfoil data*. Courier Corporation, 1959.
[26] R. M. Hicks and P. A. Henne, "Wing design by numerical optimization," *Journal of Aircraft*, vol. 15, no. 7, pp. 407–412, 1978.
[27] M. Drela, "Xfoil: An analysis and design system for low reynolds number airfoils," in *Low Reynolds Number Aerodynamics*. Springer, 1989, pp. 1–12.

Xin Fei is a Ph.D. candidate of the Operational Research and Management Science Group at Warwick Business School, University of Warwick. His research interests mainly lie in efficient information collection and stochastic optimisation.

Jürgen Branke (M'02) received his Ph.D. degree from University of Karlsruhe, Karlsruhe, Germany, in 2000. He is a Professor of Operational Research and Systems with the Warwick Business School, University of Warwick, Coventry, U.K. He has been an active researcher in the area of evolutionary optimization since 1994 and has published more than 170 papers in international peer-reviewed journals and conferences. His research interests include multiobjective optimization, handling of uncertainty in optimization, dynamically changing optimization problems, simulation-based optimisation and the design of complex systems. He is area editor of the Journal of Heuristics and the Journal on Multi-Criteria Decision Analysis, as well as associate editor of IEEE Transactions in Evolutionary Computation and the Evolutionary Computation Journal.

Nalân Gülpınar is currently an Associate Professor in Operational Research and Management Sciences at Warwick Business School, The University of Warwick, U.K. She received BSc and MSc degrees in Mathematics and a PhD in Operational Research. Before joining Warwick, she was first a research fellow, then a research lecturer in the Department of Computing at Imperial College London. Her research projects have been of multi-disciplinary nature owing to the different broad contexts in which mathematical modeling and operational research techniques are applied to develop robust and optimal decisions. The main focus has been decision-making under uncertainty and risk management with applications to various areas.